



ELSEVIER

Available online at www.sciencedirect.com**ScienceDirect**journal homepage: www.elsevier.com/locate/issn/15375110

Research Paper

On-line crop/weed discrimination through the Mahalanobis distance from images in maize fields



Iván D. García-Santillán ^{a,b,*}, Gonzalo Pajares ^a

^a Department of Software Engineering and Artificial Intelligence, Faculty of Informatics, Complutense University, Madrid, Spain

^b Department of Software Engineering, Universidad Técnica del Norte, Ibarra, Ecuador

ARTICLE INFO

Article history:

Received 20 July 2017

Received in revised form

25 September 2017

Accepted 8 November 2017

Keywords:

Crop/weed discrimination

Mahalanobis distance

Image segmentation

Machine vision

This study proposes a new automatic method for crop/weed discrimination in images captured in maize fields during the initial growth stages. The images were obtained under perspective projection with a camera installed on board at the front part of a tractor. Different approaches have addressed the problem based on crop row determination and then assuming that inter-row plants are weeds. Nevertheless, an important challenge is the identification of weeds intermixed within the crop rows. This issue is addressed on this paper by applying a minimum criterion distance based on the Mahalanobis distance derived from a Bayesian classification approach, this makes the main contribution. The identification of both intra- and inter-row weeds is useful for more accurate weed quantification for site-specific treatments. Image quality is affected by uncontrolled lighting conditions in outdoor agricultural environments. Also, different plant densities appear due to different growth stages affecting the crop/weed identification process. The proposed method was designed to deal with the above undesired situations, consisting of three phases: (i) segmentation, (ii) training and (iii) testing. The three phases are executed on-line for each image, where training is specific of each single image, requiring no prior training, as it is usual in common machine learning-based approaches, mainly supervised. This makes the second research contribution. The performance of the proposed approach was quantitatively compared against three existing strategies, achieving an accuracy of 91.8%, pixel-wise determined against ground-truth images manually built, with processing times ≤ 280 ms, which can be useful for real-time applications.

© 2017 IAgrE. Published by Elsevier Ltd. All rights reserved.

1. Introduction

1.1. Problem statement

Machine vision systems applied to agricultural tasks have great potential, as explained in Brosnan and Sun (2002) and

Davies (2009). The use of technology, including machine vision systems, in agricultural applications can reduce manual tasks and the cost of crop production (Barreda, Ruiz, & Ribeiro, 2009), and can contribute to the productivity and competitiveness of farmers to ensure agricultural supplies. Moreover, the use of traditional farming methods sometimes

* Corresponding author. Department of Software Engineering and Artificial Intelligence, Faculty of Informatics, Complutense University, Madrid, Spain.

E-mail addresses: idgarcia@utn.edu.ec (I.D. García-Santillán), pajares@ucm.es (G. Pajares).

<https://doi.org/10.1016/j.biosystemseng.2017.11.003>

1537-5110/© 2017 IAgrE. Published by Elsevier Ltd. All rights reserved.

Nomenclature	
Abbreviations	
AES	algorithm based on thresholding and morphological operations
CIVE	colour index of vegetation extraction
COM	Combination of green indices
ExG	excess green
ExR	excess red
ExGR	excess green minus excess red index
LPG	liquefied petroleum gas
LVQ	algorithm based on learning vector quantisation
NDI	normalised difference index
ODMD	on-line discrimination by Mahalanobis distance
RHEA	robotics and associated high-technologies and equipment for agriculture and forestry
ROI	region of interest
SVM	algorithm based on support vector machine
VEG	vegetative index
Symbols	
a, b, d	coefficients for the quadratic polynomial
c	pixels belonging to crop class
\bar{C}	3-dimensional vector containing $\bar{R}_c, \bar{G}_c, \bar{B}_c$
D_M^2	Mahalanobis distance squared
D_c	Mahalanobis distances for crop class
D_w	Mahalanobis distances for weed class
$Height_{(ROI)}$	height of the ROI in pixels
k	Kappa coefficient
l	length in pixels
$L1, L2, L3, L4$	crop rows labelled from left to right
m, e	slope and intercept of the straight line respectively
n	number of pixels of the class
$Margin_{(base)}$	width in pixels at the base of the ROI
$Margin_{(top)}$	width in pixels at the top of the ROI
R, G, B	RGB (red, green and blue) spectral channels
$\bar{R}, \bar{G}, \bar{B}$	average for each spectral component R, G, B
$\bar{R}_c, \bar{G}_c, \bar{B}_c$	$\bar{R}, \bar{G}, \bar{B}$ pixels representing the crop class
$\bar{R}_w, \bar{G}_w, \bar{B}_w$	$\bar{R}, \bar{G}, \bar{B}$ pixels representing the inter-row weed class
μ	vector (centroid) containing $\bar{R}, \bar{G}, \bar{B}$
w	pixels belonging to weed class
\bar{W}	3-dimensional vector containing $\bar{R}_w, \bar{G}_w, \bar{B}_w$
x, y	independent and dependent variables of the straight line, respectively
(X, Y)	pair of variables of the spectral components (R, G, B)
\bar{X}, \bar{Y}	pair of variables of the average spectral components ($\bar{R}, \bar{G}, \bar{B}$)
z	3-dimensional vector containing R, G, B spectral components

may lead to indiscriminate use of chemicals (herbicides, fertilisers), increasing production costs, soil depletion and environmental pollution (Astrand & Baerveldt, 2005; Kataoka, Kaneko, Okamoto, & Hata, 2003).

Process automation is gaining an important relevance today. In this regard, crop/weed discrimination based on images has currently received special dedication in precision agriculture. Indeed, plants located inside the inter-row spaces can be considered with very high probability to be weeds, requiring site-specific treatments (Emmi, Gonzalez-de-Soto, Pajares, & Gonzalez-de-Santos, 2014; RHEA, 2014). The intra-row weed identification is important too. However, this task is complex because crops and weeds located in the intra-crop row space are intermixed and overlapped, with a high degree of similarity in their spectral signatures.

Image quality is affected by uncontrolled lighting conditions (sudden shadows, excessive or poor illumination) in outdoor agricultural environments. Also, different plant heights and volumes due to growth stages affect the crop/weed identification process. Several solutions have been proposed to cope with the above adverse situations with the aim of discriminating between crops and weeds (Ahmed, Al-Mamun, Bari, Hossain, & Kwan, 2012; Guerrero, Pajares, Montalvo, Romeo, & Guijarro, 2012; Montalvo et al., 2012b; Tellaeche, Pajares, Burgos-Artizzu, & Ribeiro, 2011). However, because of the intrinsic difficulty involved in outdoor agricultural environments, an extra research effort is still required; mainly to discriminate crops and weeds without requiring an off-line exhaustive training process as occurs with supervised learning-based techniques. In addition, it

must be considered that an additional benefit of an on-line trained system is that it can adapt to local variations in the field, minimising the local vulnerability produced by global and off-line training system (Midtiby, 2012, p. 88).

According to the above considerations, a new strategy based on a machine vision system was designed for crop/weed discrimination in wide row crops (maize fields) at initial growth stages (up to 40 days), focused on weeds intermixed with crops in the intra-row space, by applying a minimum criterion distance based on the Mahalanobis distance derived from a Bayesian classification approach. This makes the main contribution. The method proposed was designed to deal with the above mentioned adverse environmental conditions focusing on its performance in terms of accuracy and efficiency, measured through the corresponding analysis of the confusion matrix and the Kappa coefficient.

The image processing consists of three phases, which are executed on-line for each image, where the classical training required by the Bayesian classifier is applied exclusively on each single image, requiring no prior training with a set of selected images. This makes the second research contribution. In addition, the method identifies separately weeds located on the inter- and intra-row spaces in both curved and straight crop rows (García-Santillán, Guerrero, Montalvo, & Pajares, 2017a, b).

The idea comes from the RHEA (2014) project, in which one of the tractors in the fleet was dedicated to apply site-specific treatments on maize fields, where the detection of weed pressure was an essential objective. This tractor was equipped with an automatic mechanical/thermal tool, based on

Liquefied Petroleum Gas (LPG) to destroy up to 90% of weeds by applying different levels of flaming without destroying the crops and saving the maximum amount of LPG. In this regard, it is crucial to determine weed densities with the maximum accuracy as possible to apply the correct doses based on the automatic detection process. The determination of these densities requires the identification of intra and inter-weeds patches (Gonzalez-de-Santos et al., 2016). Nevertheless, the proposed approach is also applicable in different agricultural contexts involving wide-row crops requiring different treatments such as herbicides.

The proposed strategy exploits the performance of some partial image-based procedures involved in existing methods and includes new procedures integrated on the proposed global strategy to achieve a valid procedure for crop/weed (inter and intra) discrimination with maximum accuracy as possible.

1.2. Review of methods

This section is devoted to the review of methods for crop/weed identification in the context of agricultural tasks, determining the starting point of this research. The different techniques are based on visible spectral-index, threshold, learning and wavelet (Guijarro, Riomoros, Pajares, & Zitinski, 2015).

1.2.1. Visible spectral-index based methods

These methods aim to obtain a grayscale image with high contrast highlighting the vegetation, i.e. with pixels brighter for plants and darker for soil and waste. These techniques were designed to cope with the variability of natural daylight illumination. Woebbecke, Meyer, Vonbargen, and Mortensen (1995) analysed several contrast indices in colour images. Excess green (ExG) index proved to be better for this purpose, including for sunny days with and without shadows. Kataoka et al. (2003) used the colour index of vegetation extraction (CIVE) to segment the crop of beans and sugar beet under zenithal view. Camargo-Neto (2004) combined the excess green ExG and the excess red ExR (originally proposed by Meyer, Hindman, & Lakshmi, 1998) to create a new index, known as excess green minus excess red index (ExGR). Pérez, López, Benloch, and Christensen (2000) created the normalised difference index (NDI), which uses a quotient to distinguish plants from other elements. A comparative among the indices ExG, ExGR and NDI can be found in Meyer and Camargo-Neto (2008). Ribeiro, Fernandez-Quintanilla, Barroso, and Garcia-Alegre (2005) used a linear combination of spectral components whose coefficients were obtained by using genetic algorithms. Hague, Tillett, and Wheeler (2006) described an approach to automatic estimate a density map of weed and crop using the vegetative index (VEG). Guijarro et al. (2011) used a linear combination (COM) of four vegetation indices with different contributions each. Montalvo, Guijarro, Guerrero, and Ribeiro (2016) obtained an enhanced grayscale image combining five vegetation indices and reducing the number of variables by using principal component analysis.

1.2.2. Threshold-based procedures

These methods commonly assume a two-class problem where plants and soil should be identified. Otsu (1979)

maximised the interclass variance of the plant and background pixels. It gives a threshold which is self-adjustable, performing appropriately in images captured under different conditions of illumination. Burgos-Artizzu, Ribeiro, Guijarro, and Pajares (2011) discriminated the weeds and crop using a vegetation index through a linear combination and the grayscale image was binarised using the mean intensity value. Montalvo et al. (2013) used a linear combination of three vegetative indices and then applied a double Otsu thresholding. The first thresholding separates the vegetation from the soil, and the second one separates maize plants from weeds. Romeo et al. (2013a) proposed an expert system to identify greenness inspired by a fuzzy clustering classification approach, which consists of two phases: (i) learning, to determine a dynamic threshold for each image and (ii) classification, where a simple decision making process is applied. Gee, Bossu, Jones, and Truchetet (2008) presented a method for estimating the amount of weeds in a cereal crop. The discrimination was carried out by applying segmentation region-based through colour analysis and spatial similarity in pixels.

1.2.3. Learning-based approaches

These methods are carried out through supervised and unsupervised learning processes. The training and classification phases are generally off-line and on-line processes, respectively. In the supervised approach, the support vector machines (SVM) technique was used in several studies. Guerrero et al. (2012) identified plants in maize fields, separating pixels (R, G, B) into two classes (unmasked and masked plants). Tellaeche et al. (2011) used a database (knowledge-base) containing samples previously classified. The performance was evaluated through the correct classification percentage and Yule coefficient. Ahmed et al. (2012) classified weeds and crop by using 14 features which characterise crops and weeds in images. Regarding the unsupervised approach, Montalvo et al. (2012b) used a double thresholding and LVQ (Learning Vector Quantisation) to separate weeds and crops. The fuzzy clustering technique was used by Romeo et al. (2012) to separate the green plants from the soil; Meyer, Camargo-Neto, Jones, and Hindman (2004) applied ExR and ExG to segment regions of interest; Guijarro et al. (2011) to differentiate two types of plants (crops and weeds), first discriminating plants and soil and then crop and weeds in the plants. Nieuwenhuizen, Hofstee, and van Henten (2010) developed an adaptive Bayesian classifier to classify volunteer potato plants in sugar beet field, where crop row information was used to train the classifier, without having to choose training data beforehand.

1.2.4. Wavelet-based techniques

In agricultural image processing sometimes is required to highlight details (edges) and to detect textures by analysing the image from different angles. Thus, two categories are established:

- 1) Analysis on the frequency content, considering the image as a signal to separate low (smooth variations in colour) and high frequency components (edges which give details). Bossu, Gee, Jones, and Truchetet (2009) discriminated crop

- and weeds applying the wavelet transform and comparing the performance of four families of waves.
- 2) Textures (characteristics) analysis under the assumption that different plants (crop and weeds) respond in a different way to low/high pass filtering. [Guizarro et al. \(2015\)](#) proposed a method for distinguishing soil and vegetation, combining the greenness of plants by applying ExG and the texture spatial information through the wavelet transform and statistical descriptors of first order (e.g. mean and standard deviation). [Chou, Chen, and Yeh \(2007\)](#) identified the crop by using wavelet packet transform combined with weighted Bayesian distance based on crop texture and leaf features. They computed energy coefficients in several frequency bands, obtained after the transformation, to make plants discrimination. [Ishak, Hussain, and Mustafa \(2009\)](#) used a combination of a Gabor wavelet (filters) with gradient field distribution to identify different types of weeds under the assumption that grasses, broadleaves and narrow leaves display different features.

Based on the review of methods, some approaches have provided useful insights which are exploited to design the proposed approach, they are the following: a) vegetation indices to highlight the greenness in a grayscale image; b) thresholding to obtain a binary image and to separate the pixels belonging the soil and vegetation; c) centroids of the crop and weed classes for classifying pixels.

2. Materials and methods

2.1. Images collection system

The images used for this study belong to maize crops. They were captured with a Panasonic DMC-SZ8 colour camera installed on board a tractor on its front part at two experimental sites with a total surface of 3 ha: southern of Madrid near of the Manzanares's riverside and CSIC-CAR facilities on La Poveda Research Station, Arganda del Rey, Madrid-Spain. A set of more than 3000 images were acquired in April/May/June during each year between 2013 and 2017. The acquisitions were spaced approximately by six days during a period of 40 days at the different years, i.e. they were obtained under different environmental lighting conditions and different growth stages in maize and weed plants. [Figure 1](#) shows illustrative examples of the images captured on the field. A sunny day with high density of weeds is shown in (a), cloudy day with medium level of weeds in (b) and intermediate day with low pressure of weeds in (c). Images in (a)–(c) contain only straight crop rows and (d) curved crop rows.

The digital images were captured under perspective projection and stored as 24-bit colour images with resolutions of 1920 × 1080 pixels saved in RGB colour space in the JPEG format. The pitch (inclination) angles ranging between 20° and 30° and heights between 1.50 and 2.30 m from the ground with the aim of focusing the region of interest (ROI) where the site-specific treatments are to be applied. The focal length in the optical system was ranging between 6 and 9 mm. The size and location of the ROI was specified considering the following: (i)

the number of crop rows to be detected and (ii) the imaged ROI that contains enough resolution (in pixels) to identify unambiguously green plants (crop and weed) from soil ([Pajares et al., 2016; Romeo et al., 2013b](#)). In the proposed approach four crop rows were selected for detection, which is the number used in the [RHEA \(2014\)](#) project and reported by [Emmi et al. \(2014\)](#) because the implement applying LPG had four couples of burners, each couple acting on a crop row. Considering the four crop rows and the inter-row space of 0.75 m the total width of the ROI is 3 m. This area starts at 3 m with respect to a virtual vertical axis traversing the centre of the image plane in the camera. This value avoids that the elements in front of the tractor are imaged. The length was fixed to 4 m because it provides sufficient image resolutions as explained above. This 3D area in the field results in an image resolution of 1500 × 600 pixels (width × height), which represents approximately the 43% of the full original image and is always located at the same position inside the image. [Figure 2\(a\)](#) shows an example of the ROI enclosed in the rectangle on crop rows. Nevertheless, the method can be easily adapted for detecting any number of crop rows with the corresponding camera setting.

The images were processed with Matlab from [MathWorks \(2015\)](#), release 8.5 (R2015a), using an Intel Core i7 2.0 GHz processor (4th generation), 8 GB RAM, Windows 8.1 Pro operating system (64-bits).

2.2. Image processing method architecture

The proposed method consists of three main phases: (i) segmentation, (ii) training and (iii) testing. [Figure 3](#) shows the full structure, including the flow chart. All phases are executed on-line, i.e. with the corresponding processes running on real time, so that the input data from each image are acquired, updated and processed immediately.

This method was designed to run as a subsequent stage to the crop rows detection process, i.e. once each crop row has been described by its corresponding equation (polynomial) as straight ($y = mx + e$) or quadratic ($y = ax^2 + bx + d$) line within the ROI ([Fig. 2a](#)). At each straight line, the estimated coefficients m and e are the slope and intercept respectively, whereas in the quadratic line the variables are a , b and d , where ' a ' is the coefficient of curvature. In both straight and quadratic polynomials, x and y are the independent and dependent variables, respectively. [Figure 2\(b and c\)](#) display the ROI with four straight and curved crop rows previously detected (red lines) using the method proposed by [García-Santillán et al. \(2017b\)](#) due to its simplicity and performance. This method determines the locations and coefficients of the straight and quadratic crop rows by using the Hough transform (HT) and the micro-ROI concept to explore pixel alignments that belong to the crop row, obtaining several significant points located along the potential crop rows. Then, regression analysis by squared least is applied to fit such points to straight and quadratic polynomials. Finally, the better polynomial (straight or quadratic) for each crop row is selected based on a minimum norm of residues criterion. In this paper, the number of crop rows is restricted to four as explained above, which cross the base of the ROI. This number is sufficient for automatic vehicle guidance and weeds



Fig. 1 – Illustrations of images processed by the method under different lighting conditions, weeds densities and plant sizes; (a) sunny day with a high level of weeds; (b) cloudy day with medium density of weeds and (c) intermediate day with low pressure. In (a)–(c), images containing straight crop rows and (d) with curved crop rows.

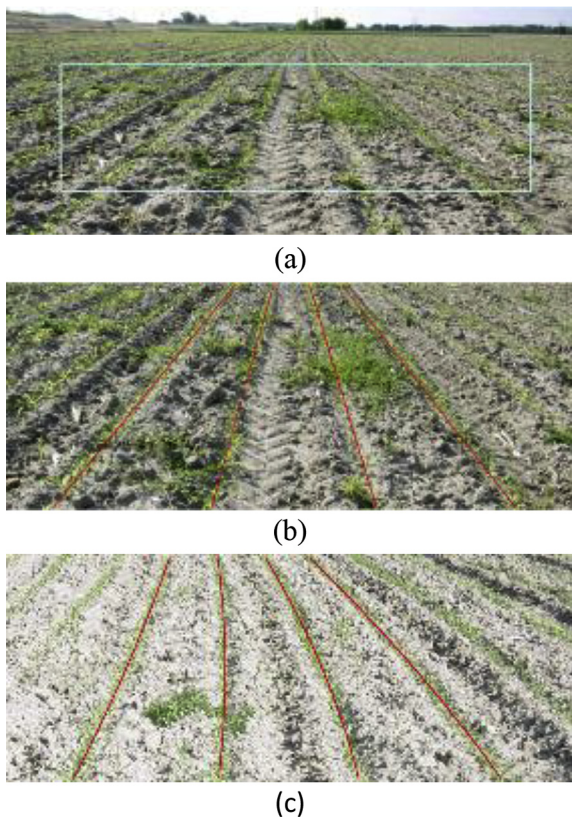


Fig. 2 – (a) Delimitation of the ROI (in rectangle) in the original RGB image; (b, c) Examples of ROI with four straight and curved crop rows detected by using García-Santillán et al. (2017b).

identification, as justified in RHEA (2014) project. The problem of straight and curved crop rows detection has been successfully addressed by applying several approaches, namely: Hough transform, linear regression, exploration horizontal

stripes, accumulation of green pixels, vanishing point, frequency analysis, blob analysis, vision stereo and regular patterns (Montalvo et al., 2012a; Guerrero et al., 2013; Vidović, Cupec, & Hocenski, 2016; García-Santillán et al., 2017a, b).

The proposed method was designed taking into account prior knowledge about straight and curved crop rows detection and crop/weed discrimination, acquired during previous works addressing this topic and based on several constraints, also derived from previous experiences. Knowledge and constraints are summarised as follows:

- In images, crops and weeds display a high degree of similarity in their spectral signatures (similar green colours), but still with sufficient differences for separation, based on image segmentation.
- A crop row in the image is an accumulation of green pixels following specific alignments (straight or curved).
- During the time of treatment in maize fields, at relatively early growth states, the weeds appear on isolated patches with respect to the crops and irregularly distributed in the field with different densities in the inter- and intra-row spacing.
- The intrinsic and extrinsic parameters related to the geometry of the visual system are known.
- The method must work under the different adverse environmental conditions expressed above.

Below the main phases of the proposed method are detailed.

2.3. Segmentation

Discrimination, with the maximum accuracy as possible in wide crop rows, between crops and weeds with similar spectral signatures is crucial for site-specific treatments in precision agriculture. In this regard, the automatic Otsu-based approach, used by Montalvo et al. (2013), applying a double

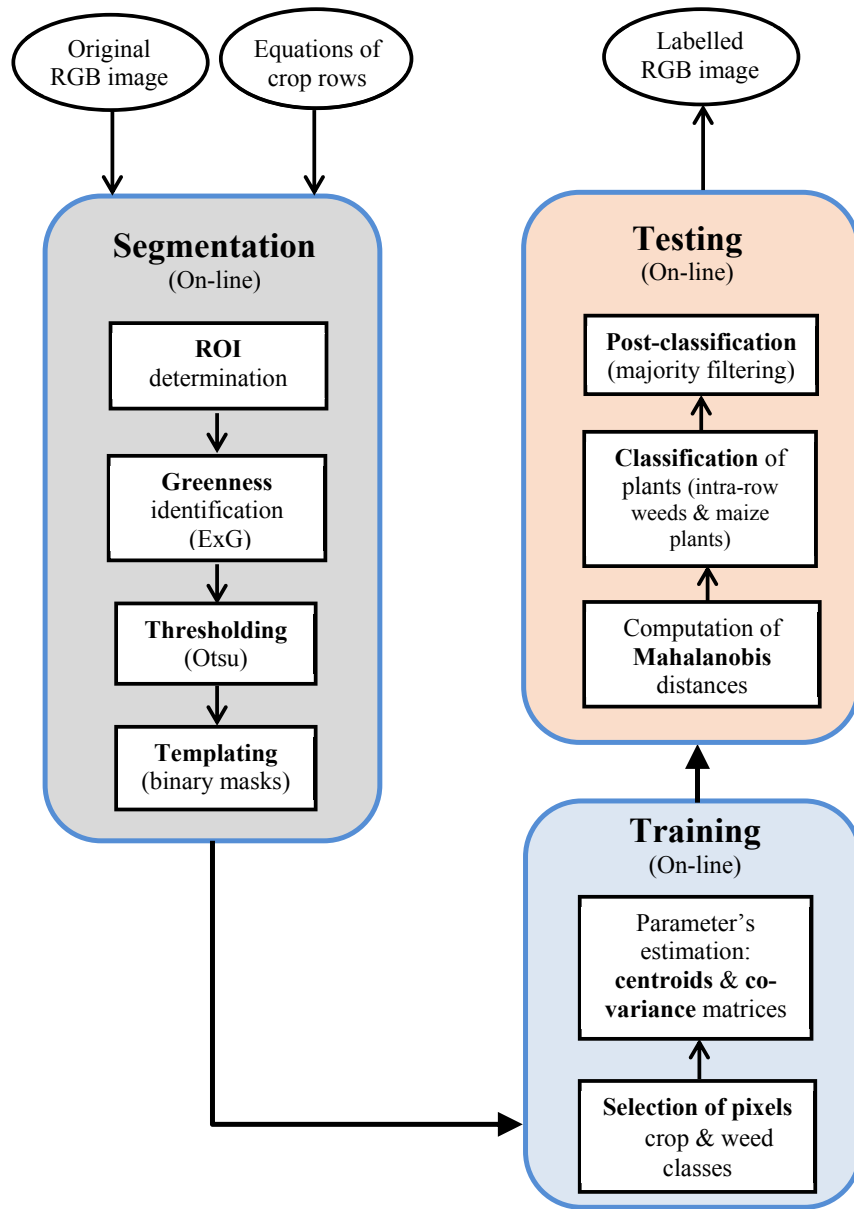


Fig. 3 – Image processing method architecture.

thresholding has gained in performance against other existing strategies such as the ones involving supervised learning as the support vector machines (Guerrero et al., 2012). The supervised methods require exhaustive training, unlike the thresholding, which has the ability of self-adjusting to the highly changing environmental conditions common in outdoor agricultural environments. Under these considerations, the segmentation phase was designed with the following four processes: (a) ROI determination; (b) greenness identification; (c) thresholding and (d) templating. The segmentation phase produces two binary images called masks (or templates) to limit spaces on the image where pixels belong to crops and weeds respectively.

2.3.1. ROI determination

As specified above in section 2.1. Figure 2(a) shows a ROI enclosed in the rectangle.

2.3.2. Greenness identification

The ExG index (Woebbecke et al., 1995) was selected because of its performance after exhaustive studies with different indices (Guijarro et al., 2011) without apparent improvements. Figure 4(a and b) show the resulting grayscale images after applying ExG to each ROI on straight and curved crop rows respectively. ExG index is defined as follows:

$$\text{ExG} = 2g - r - b \quad (1)$$

where r , g and b are the chromatic components obtained as follows:

$$r = \frac{R_n}{R_n + G_n + B_n}, g = \frac{G_n}{R_n + G_n + B_n}, b = \frac{B_n}{R_n + G_n + B_n}, \text{with } r + g + b = 1 \quad (2)$$

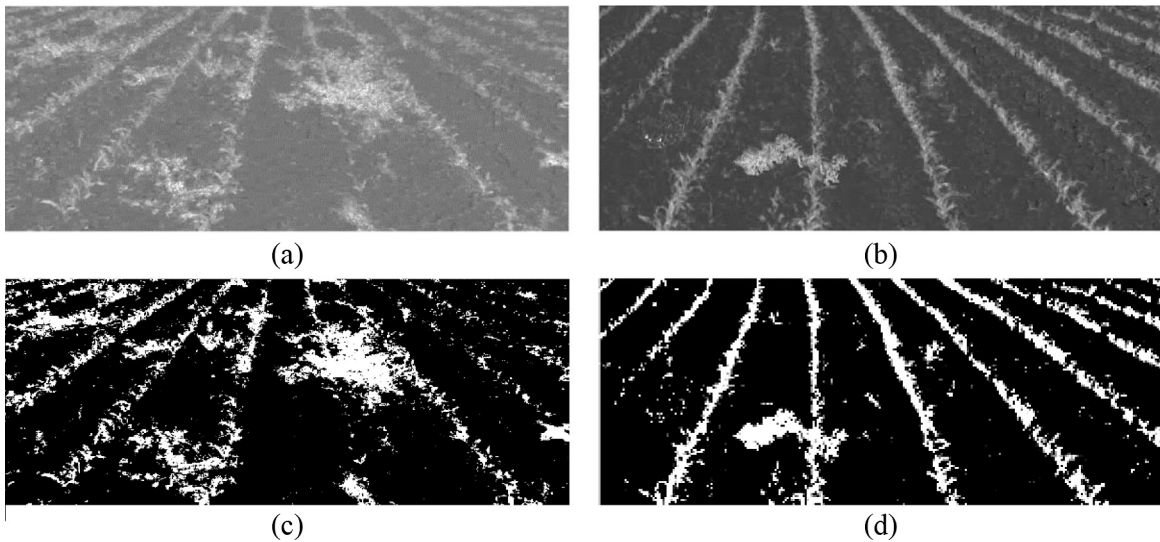


Fig. 4 – (a, b) Greyscale images after applying ExG; (c, d) binary images after applying the Otsu-based thresholding.

where R_n , G_n and B_n are the normalised RGB spectral channels ranging [0, 1] and computed as follows:

$$R_n = \frac{R}{R_{\max}}, G_n = \frac{G}{G_{\max}}, B_n = \frac{B}{B_{\max}} \quad (3)$$

where R_{\max} , G_{\max} , B_{\max} are the maximum values in the corresponding spectral channels.

2.3.3. Thresholding

Given a grayscale image after the ExG application, a unique thresholding is applied to separate green plants (crops and weeds) from soil. The thresholding process is based on the Otsu's method (1979) because of its well-tested performance in different scenarios including agricultural environments (Guijarro et al., 2015; Montalvo et al., 2016). Figure 4(c and d) show each ROI as a binary image containing green plants (crops/weeds) with similar spectral signatures labelled in white against the background in black.

2.3.4. Templating

Based on the crop rows equations ($y = mx + e$; $y = ax^2 + bx + d$) (Fig. 2b and c), the crop rows are labelled from left to right as L1, L2, L3 and L4 respectively. Then, margins of equal size are established for each crop row. Figure 5(a and b) show the crop rows estimated (in red) with their respective margins bounded by yellow lines. Because of image perspective projection, the same distance in the field is imaged with different dimensions in pixels on the image, i.e. $\text{Margin}_{(\text{base})}$ and $\text{Margin}_{(\text{top})}$ at the bottom and top of the image, respectively. Considering the number of horizontal lines of the ROI ($\text{Height}_{(\text{ROI})}$) and starting on the base with a width of $\text{Margin}_{(\text{base})}$ at each horizontal line, the width decreases a magnitude l given by Eq. (4) with respect to the previous horizontal line.

$$l = \frac{\text{Margin}_{(\text{base})} - \text{Margin}_{(\text{top})}}{\text{Height}_{(\text{ROI})}} \quad (4)$$

where as described above $\text{Margin}_{(\text{base})}$ is the width at the base of the ROI, $\text{Margin}_{(\text{top})}$ the width at the top of the ROI and

$\text{Height}_{(\text{ROI})}$ the height of the ROI, all measured in terms of number of pixels. The first two parameters are established according to the crop growth stage. In this study, the margin at the base of the ROI was established by experimentation between 100 and 160 pixels, corresponding to 15 and 25 cm respectively in the 3D space (maize field). With such purpose, the crop row width was measured (in cm) in the 3D space and then transformed into pixel units into the 2D image, with the prior knowledge of the camera system geometry (Pajares et al., 2016). The margin at the top of the ROI was set at 30% of the previous value according to the geometric configuration used in the machine vision system.

Once margins are established (Fig. 5a and b), two binary images (masks) are created. The first mask contains white pixels located inside the four margins (intra-crop space), Fig. 6(a and b). The second mask is complementary and contains white pixels located outside of the margins, i.e. on the inter-row spaces, Fig. 6(c and d).

The idea of applying binary masks to limit where pixels belong to the crop was used by Montalvo et al. (2012a), where masks are manually built off-line by applying knowledge about camera settings and visual system geometry. On the contrary, in the proposed method, masks are dynamically built for each image, according to the main idea of off-line processing guiding this research.

2.4. Training

Given two binary masks obtained in the previous phase (inter and intra-row spaces), two on-line processes are also carried out to select pixels belonging to two classes (crops and weeds). Without loss of generality, it is assumed that samples on both classes can be modelled as Gaussian probability density functions (Duda, Hart, & Stork, 2001), which are defined by two parameters each of them, i.e. mean or centroid and co-variance matrix. These parameters are to be estimated, based on the selection of samples, as described below:

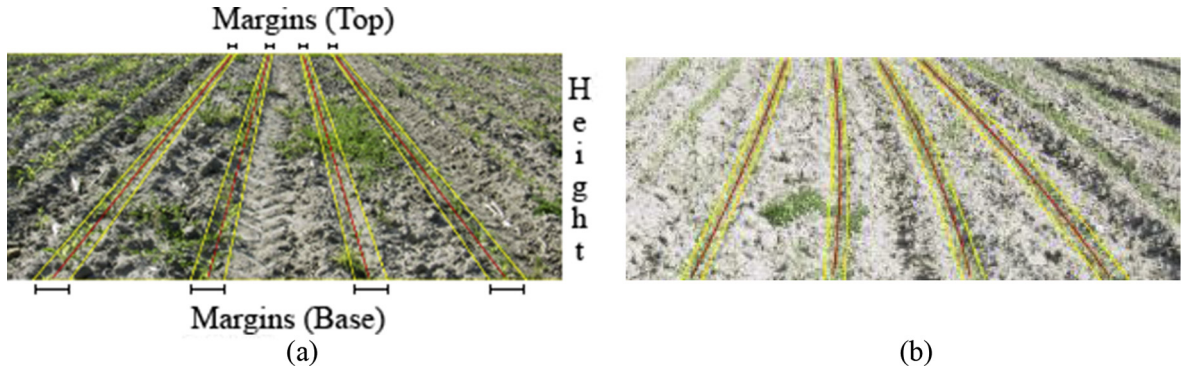


Fig. 5 – Illustrations of the ROI with four crop rows estimated (in red) and the respective margins (in yellow). In (a) and (b) on straight and curved crop rows, respectively.

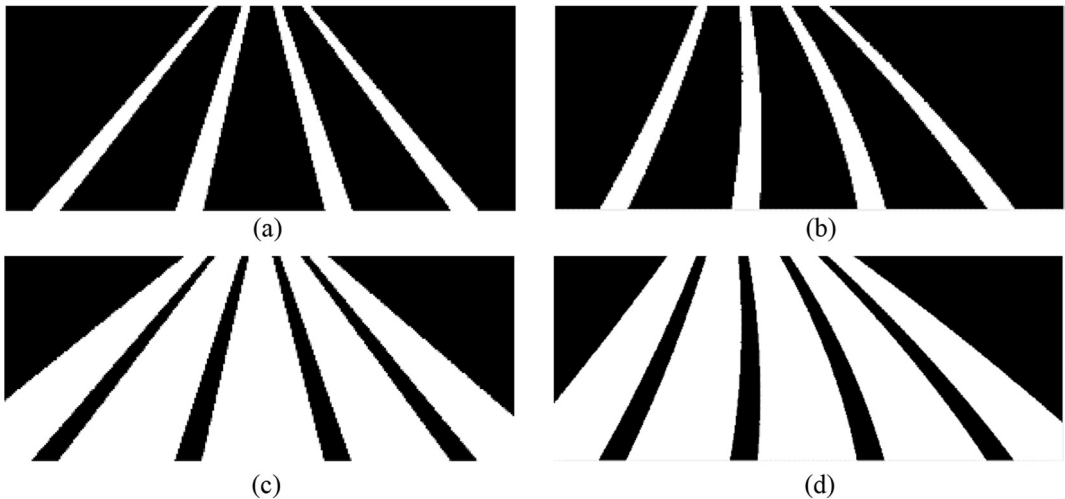


Fig. 6 – Binary images (masks); (a, b) masks containing four margins on straight and curved crop rows respectively; (c, d) masks containing inter-rows spaces.

2.4.1. Selection of pixel samples for each crop/weed class

With the binary masks available, a logical AND operation is carried out with the binary image containing the vegetation (e.g. Fig. 4c). It is assumed that majority of pixels belonging to weeds are on the inter-crop row space and the majority of pixels belonging to crops are on the intra-crop row. The following explanation is based on representative figures for illustrative purposes. The mask in Fig. 6(c) is used to identify the sample of inter-row weeds (Fig. 7a) by applying a logical AND operation between Fig. 4(c) and Fig. 6(c). Likewise, the mask in Fig. 6(a) is used to identify the sample of intra-row crops and weeds (Fig. 7c) by applying a logical AND operation between Fig. 4(c) and Fig. 6(a). White pixels on the resulting binary images provide pixel locations on the original ROI containing RGB spectral values, which are the samples $x \in R^3$ for parameter's estimation (centroid and co-variance matrices).

2.4.2. Parameter's estimation: centroids and co-variance matrices

The centroid is defined as a vector containing the average for each spectral component R, G, B:

$$\mu = (\bar{R}, \bar{G}, \bar{B})$$

$$\bar{R} = \frac{1}{n} \sum_{i=1}^n R_i, \bar{G} = \frac{1}{n} \sum_{i=1}^n G_i, \bar{B} = \frac{1}{n} \sum_{i=1}^n B_i \quad (5)$$

where R, G, B are the spectral red, green and blue components respectively and n is the number of pixels belonging to the class.

The co-variance matrix is a square and symmetric matrix (3×3) containing the variances and co-variances associated with the three spectral components. The elements in the main diagonal of the matrix contain the variances of the components $x = (R, G, B)$, while the elements outside the diagonal contain the co-variances among all possible pairs of variables. The co-variance between two variables is defined as follows:

$$\text{Cov}(X, Y) = \left(\frac{1}{n} \sum_{i=1}^n X_i Y_i \right) - \bar{X} \bar{Y}, \forall (X, Y) \in RGB \quad (6)$$

where (X, Y) is a pair of generic variables with the three spectral components (R, G, B); \bar{X}, \bar{Y} the respective means obtained by Eq. (5) and n the number of pixels belonging to the class.

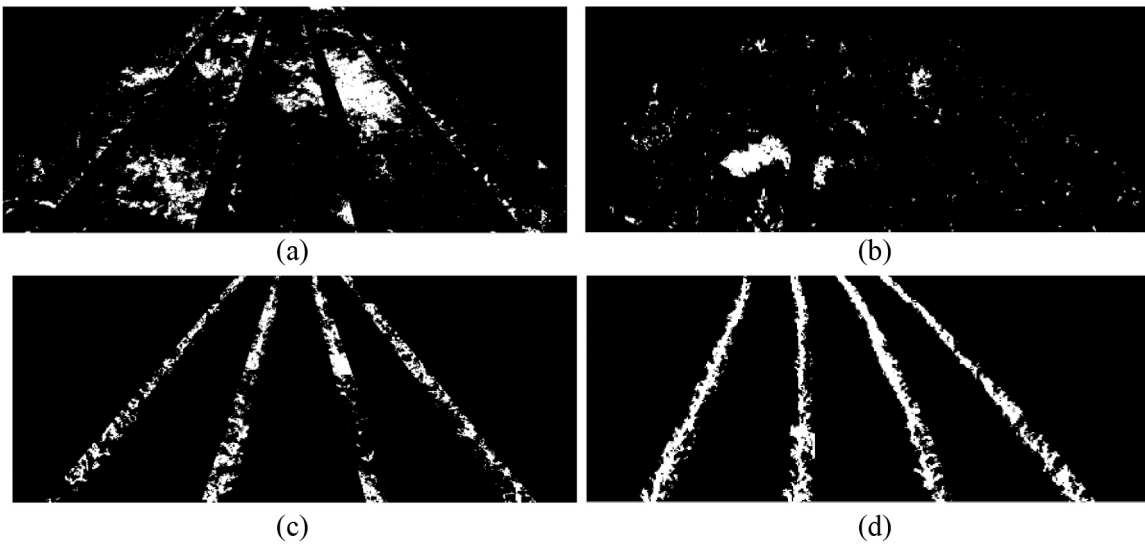


Fig. 7 – (a, b) Pixels representing the inter-row weed class on straight and curved crop rows respectively; **(c, d)** pixels belonging to the crop class, which will be refined later to discriminate between maize plants and intra-row weeds.

Two steps are carried out to compute the centroids and co-variance matrices of crop and weed classes as follows:

- RGB pixels from the ROI representing the inter-row weed class are selected, see Fig. 7(a), and then the centroid $\bar{W} = (\bar{R}_w, \bar{G}_w, \bar{B}_w)$ and the co-variance matrix are computed by using Eqs. (5) and (6) respectively. Distribution of the RGB pixels in the R^3 space belonging to the inter-row weeds with its respective centroid is displayed in Fig. 8(a), which turns out to be $\bar{W} = (145, 164, 126)$.
- RGB pixels from the ROI representing the crop class are selected from Fig. 7(c), and then the centroid $\bar{C} = (\bar{R}_c, \bar{G}_c, \bar{B}_c)$ and the co-variance matrix are computed as before. Distribution of the RGB pixels in R^3 space belonging to the crop with its respective centroid is shown in Fig. 8(b), which turns out to be $\bar{C} = (174, 190, 141)$.

In Fig. 8(a and b) it can be seen the distribution of the spectral components with a different arrangement in the three spatial directions on R^3 and without a symmetric distribution around the centroid. The Mahalanobis distance can cope with this kind of asymmetric distribution unlike the Euclidean distance which is only effective on symmetric distributions. Also, in both graphs (Fig. 8) it can be seen that there is an overlapping between crop and weed classes due to the high similarity in their spectral signatures (green colours), but still with differences for separation purposes. Different species display different greenness due to the amount of photosynthetic pigments (chlorophylls and carotenoids). These differences are translated to the images, allowing the modeling of two classes as Gaussian distributions. Table 1 shows a statistical test of sampled distributions belonging to crop and weed classes in the maize field. According to skewness and kurtosis values the data on crops and weeds classes are slightly displaced left (negative asymmetry) with a distribution similar to a bell-shaped, i.e. a normal distribution. Therefore, it can be assumed without loss of generality that

samples on both classes can be modelled as Gaussian probability density functions, each defined by two parameters, i.e. mean or centroid and co-variance matrix.

2.5. Testing

Given the centroids and co-variance matrices for each class (crop and weeds) obtained in the previous phase, three on-line steps are carried out for crop/weed discrimination, including the intra-row weeds that have not been identified yet (Fig. 7c). These processes are: (i) computation of Mahalanobis distances, (ii) classification of plants and (iii) post-classification.

2.5.1. Computation of Mahalanobis distances

[Mahalanobis \(1936\)](#) proposed a distance between a set of points and a multivariate space's centroid (overall mean). This method classifies the observations into predicted groups (weed/crop) through a measure of spectral similarity considering correlation among variables (R, G, B). The Mahalanobis distance was used instead of other measures (e.g. Euclidean distance) because of that crop and weed classes are distributed geometrically as ellipsoidal clusters instead of a sphere (see Fig. 8a and b). The R, G, B variables are not statistically independent but rather correlated. The squared Mahalanobis distance takes this into account, being the key part in the decision phase of a Bayesian classifier. It is defined as follows:

$$D_M^2 = (\mathbf{z} - \boldsymbol{\mu})^T \text{Cov}_z^{-1} (\mathbf{z} - \boldsymbol{\mu}) \quad (7)$$

where \mathbf{z} are 3-dimensional vectors containing the three R, G, B spectral values of each class (crop/weed), $\boldsymbol{\mu}$ the centroid and Cov_z the co-variance matrix defined by Eqs. (5) and (6) respectively. The squared Euclidean distance can be obtained from Eq. (7) by considering the covariance matrix as the identity matrix.

The memory and time requirements to compute the (squared) Mahalanobis distances increase quadratically with the number of variables for each observation. However, as this

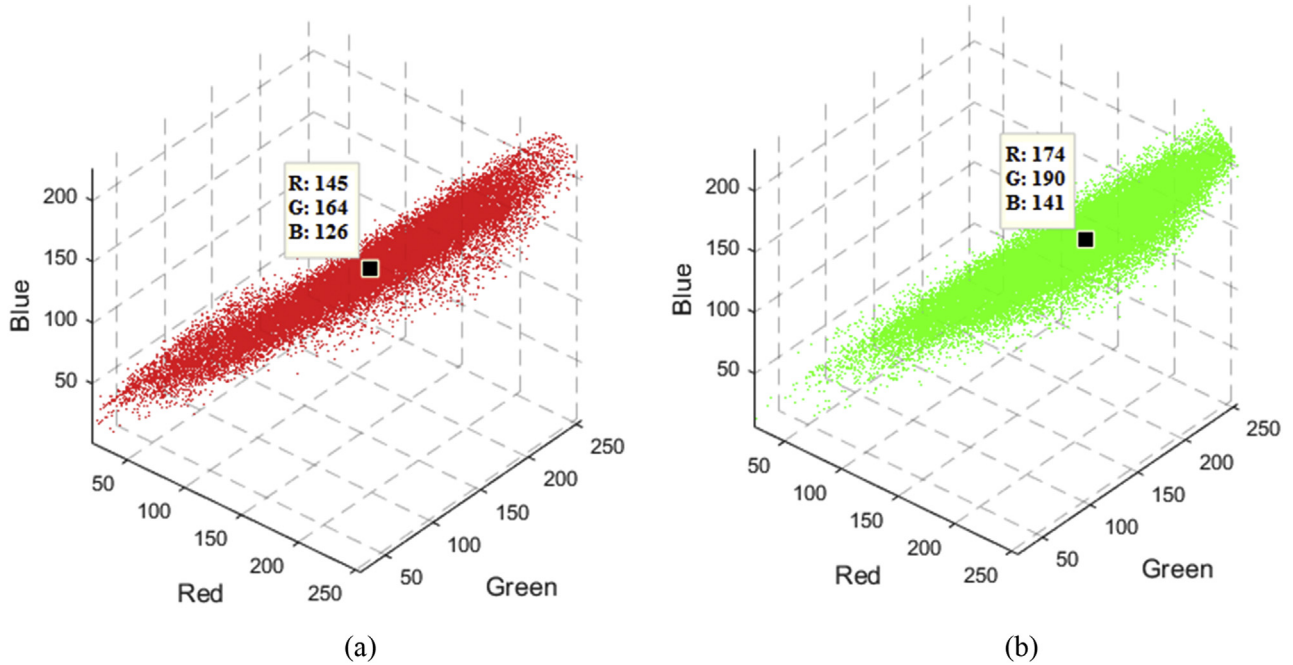


Fig. 8 – Distribution of RGB pixels in R^3 space with the respective centroid; (a) inter-row weed class; (b) crop class.

Table 1 – Statistical test of sampled distributions belonging to crop and weed classes in the maize field.

	Crop			Weed		
	R	G	B	R	G	B
Average	174	190	141	145	164	126
Std. Deviation	36.11	34.85	34.10	43.89	42.76	38.58
Skewness	-0.49	-0.59	-0.30	-0.44	-0.48	-0.25
Kurtosis	-0.25	-0.01	-0.38	-0.40	-0.37	-0.50

study deals only with the variables of spectral components (R , G , B), the computational time can be easily assumed by the method, as explained in Section 3. Mahalanobis distances for each class (crop/weed) are computed by using Eq. (7) as follows:

$$\begin{aligned} D_w &= D_M^2(c, \bar{W}), \forall c \in \text{crop class} \\ D_c &= D_M^2(c, \bar{C}), \forall c \in \text{crop class} \end{aligned} \quad (8)$$

where c depicts the pixels belonging to crop class, \bar{W} and \bar{C} the centroids obtained by Eq. (5). D_w is the distance between spectral RGB pixel values in the crop class (Fig. 8b) from the centroid of the inter-row weed class (Fig. 8a). The computed squared distances (D_w and D_c) are used in the next step for discrimination between green plants in the intra-row space, i.e. crops and weeds.

2.5.2. Classification of intra-row plants

The next step is to discriminate crops from weeds in the intra-row space (furrows) where they coexist. The data are the pixels classified as belonging to the crop rows (Figs. 7c and 8b). Based on the squared Mahalanobis distances (D_w and D_c) computed in the previous process they are used as similarity measures (Rodríguez & Sossa, 2011) and the decision rule for the intended discrimination is defined as follows:

$$\begin{aligned} &\text{if } (D_c * P(c) \leq D_w * P(w)) \text{ then} \\ &\text{Pixel} \in \text{crop} \\ &\text{else} \\ &\text{Pixel} \in \text{intra row weeds} \end{aligned} \quad (9)$$

where $P(c)$ and $P(w)$ are the a priori probabilities for crops and weeds, respectively. This allows considering prior knowledge when available with $P(c) + P(w) = 1$. In our approach it is assumed no prior knowledge and both are set to 0.5. Nevertheless, one could consider the shape of leaves by example, which are different in crops and weeds to assign different values to the a priori probabilities. At this point, three groups of pixels are identified: crop class (maize plants) and weed plants in the inter- and intra-row spaces.

2.5.3. Post-classification

In order to improve the results of the initial classification (Eq. (9)), a stage of refinement is applied on the resulting binary images by using a majority morphological filtering with a neighbourhood of 7×7 . The effect of varying the size for 3×3 and 5×5 were also studied. The filtering allows homogenising the resulting image, removing spurious pixels that usually occur in the classification of agricultural images. The filter assigns the central pixel to the category (label) with the majority of values in the neighbourhood.

Classification and refinement of pixels belonging to crop class (Fig. 7c) with applying majority filter 7×7 is shown in Fig. 9. In (a, b) intra-row weeds on straight and curved crop rows respectively and (c, d) refined crop class (only crop plants).

For illustrative purposes, three sets of pixels are identified as crops (Fig. 9c), inter-row weeds (Fig. 7a) and intra-row weeds (Fig. 9a). Figure 10 displays labels with different colours for these classes, (a) by using the Mahalanobis distance and (b) the Euclidean distance. The crop (maize plants) is labelled in blue, intra-row weeds in red and inter-row weeds

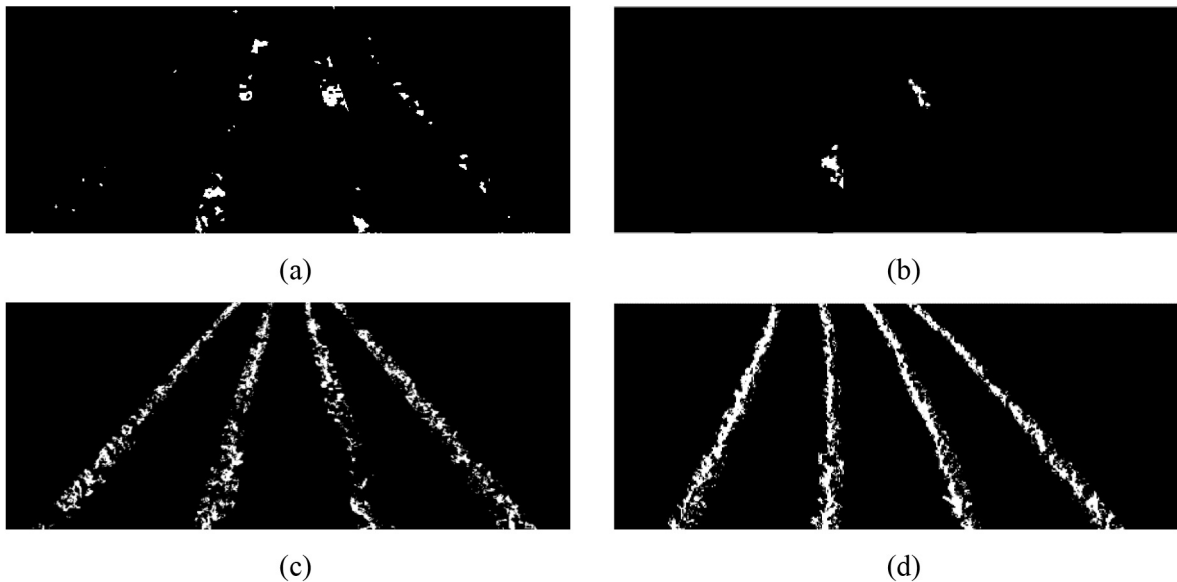


Fig. 9 – Classification and refinement of pixels belonging to crop class (Fig. 7c and d) by applying majority filtering with size 7×7 ; (a, b) intra-row weeds on straight and curved crop rows respectively; (c, d) refined crop class (only crop plants).

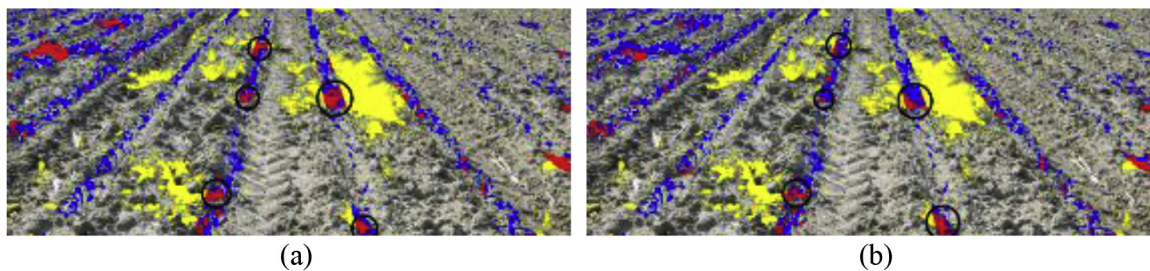


Fig. 10 – Crop/weed identification by applying (a) the Mahalanobis distance and (b) the Euclidean distance. Maize plants appear in blue, intra-row weeds in red and inter-row weeds in yellow. The main differences are shown in circles.

in yellow. The major differences by using both distances are displayed in circles.

3. Results and discussion

In order to quantitatively assess the validity of the proposed strategy, 300 original images were randomly selected with different weed densities. This sample corresponds to the 10% of images acquired, which were visually analysed by an expert to identify weeds and crops plants. The visual observation was carried out for each image guided by the segmented image through the proposed approach in this paper. The expert concentrated his major effort by identifying maize plants and both inter- and intra-row weeds. The intra-row weeds are difficult to identify because of high spectral similarity (green colours) than crops, as well as they are usually intermixed and overlapped with the crop within the furrows.

Original RGB images were manually labelled, generating a new-segmented image, considered as the ground-truth. Following the idea of Montalvo et al. (2016) in order to facilitate the creation of ground-truth and the verification process, each ROI (1500×600 pixels) was divided in 20 sub-images of

equal size (300×150 pixels) as shown in Fig. 11. The bounded area (in red) was used to generate the ground truth, i.e. 11 sub-images per ROI, which expedites the visual inspection of the expert. Thus, a total of 3300 sub-images were created, making up the ground-truth. Figure 12 illustrates an example of the ground-truth; in (a) RGB sub-image; (b) sub-image manually labelled by the expert using three labels (colours): inter-row weeds in yellow, intra-row weeds in red and crop in blue. It can be seen that even for an expert it becomes difficult to

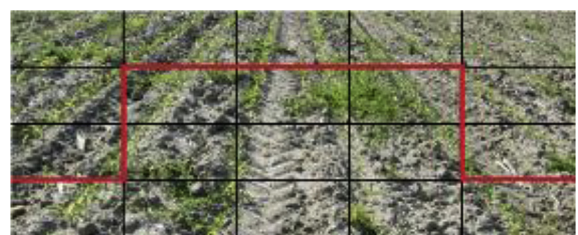


Fig. 11 – Division of the ROI (1500×600 pixels) in 20 sub-images of equal size (300×150). The bounded area (under the red line) is used to create the ground-truth, i.e. 11 sub-images per ROI.

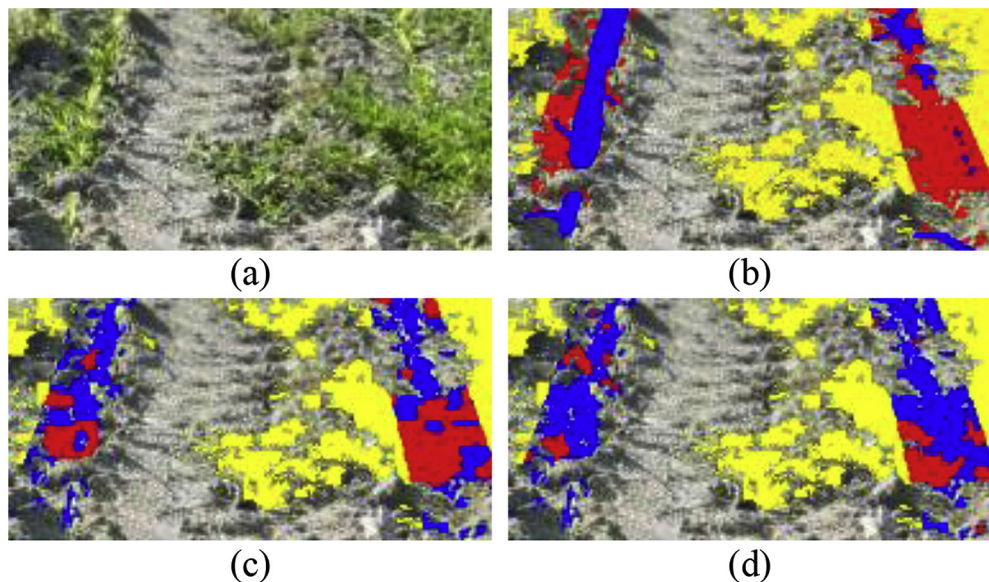


Fig. 12 – Example of the ground-truth; (a) RGB sub-image; (b) sub-image manually labelled by the expert using three labels (colours): inter-row weeds in yellow, intra-row weeds in red and crop in blue. Automatic classification of the sub-image by applying two similarity measures: (c) the Mahalanobis distance and (d) the Euclidean distance.

distinguish between pixels belonging to crop and intra-row weeds.

The evaluation of the classification was performed by analysing a confusion matrix and computing both the accuracy rate and Kappa coefficient (Bossu et al., 2009; Castillejo-González et al., 2009). Regarding the confusion matrix a bi-class classification problem is considered between crops and weeds (regardless of whether weeds are inter- or intra-row ones). The accuracy rate is the ratio between the number of correctly classified pixels and the total number of pixels, which is defined as follows:

$$\text{accuracy} = \frac{\text{TP} + \text{TN}}{\text{TP} + \text{FP} + \text{TN} + \text{FN}} \quad (10)$$

where symbols T and F mean true and false and P and N mean positives and negatives, respectively.

The Kappa coefficient (k) indicates whether the results obtained in the confusion matrix are significantly better than those produced in a random classification (Congalton, 1991). This value lies in the range [0, 1], being 1 the best score.

On average, an accuracy rate of 91.8% was obtained on the tested images by applying the Mahalanobis distance with majority filtering with size 7×7 (Table 2). Also, 87.92% and 84.23% were obtained by varying the size of the majority filtering for 5×5 and 3×3 respectively.

On average, Kappa coefficients (k) with majority filtering with sizes 7×7 , 5×5 and 3×3 were 0.77, 0.70 and 0.62 respectively. All estimated coefficients achieve a substantial degree of agreement, according to the scale proposed by Landis and Kock (1977) in Table 3. The filtering with size 7×7 outperforms results in both, accuracy measurements (91.8%) and Kappa coefficient ($k = 0.77$). This improvement can be justified because more significant compact regions are generated and the quantification of weeds for site-specific treatments becomes easier. Figure 13 shows examples of four images with the crop/weed identification by using the Mahalanobis distance and majority filtering with size 7×7 from images in Fig. 1. This classifier (7×7) works properly, satisfying the requirements of commonly accepted values higher than 85% in accuracy (Foody, 2002) and Kappa coefficient value greater than 0.70 (Montserud & Leamans, 1992). Table 4 contains an illustrative example with the confusion matrices and their respective Kappa coefficients for an image with 7×7 filter using the Mahalanobis and Euclidean distances for classification.

The refinement step by using the majority filtering improved significantly the accuracy of the initial classification on the tested images. On average, about 10% better than initial values due to the decreased misclassified pixels, mainly those belonging to the edges of maize leaves and shaded areas, which are typical in agricultural environments. Figure 14 displays an example of classification; in (a) RGB sub-image; (b) and (c) without and with refinement, respectively.

The method proposed by using the Mahalanobis distance was compared against the Euclidean distance, Figs. 10 and

Table 2 – Average accuracy rate (%) and Kappa coefficient (k) of the automatic method for the Mahalanobis and Euclidean classifiers.

Classifier	Filter	Accuracy (%)	Kappa (k)
Mahalanobis	7×7	91.8	0.77
	5×5	87.92	0.70
	3×3	84.23	0.62
	1×1	76.57	0.55
Euclidean	7×7	85.91	0.65
	5×5	82.78	0.58
	3×3	77.80	0.50
	1×1	70.73	0.44

Table 3 – Strength of agreement associate with Kappa statistics proposed by Landis and Kock (1977).

Kappa statistic	Strength of agreement
<0,00	Poor
0.00–0.20	Slight
0.21–0.40	Fair
0.41–0.60	Moderate
0.61–0.80	Substantial
0.81–1.00	Almost perfect

12(c and d). The results of the accuracy rates on tested images are shown in Table 2. On average, 85.91%, 82.78% and 77.80% were obtained by applying the Euclidean distance with majority filtering with sizes 7×7 , 5×5 and 3×3 respectively. The filtering for size 7×7 also outperforms results as occur with the Mahalanobis distance. The Kappa coefficient (k) with majority filtering for sizes 7×7 , 5×5 and 3×3 were 0.65, 0.58 and 0.50 respectively. These three results do not satisfy the

commonly accepted values regarding the accuracy (>85%) and Kappa coefficient (>0.70) as occurred with the classification based on the Mahalanobis distance with size 7×7 .

From the results in Table 2, it can be seen that the Mahalanobis approach outperforms the Euclidean one. This is in accordance with the results reported by Castillejo-González et al. (2009) and explained on the fact that crop and weed classes are distributed geometrically in ellipsoidal groupings (Fig. 8), i.e. R, G, B spectral components of pixels belonging to vegetation are not statistically independent, but rather correlated. The Mahalanobis distance takes into account this fact, as mentioned before.

Hereinafter, the proposed method for crop\weed discrimination is denoted by ODMD (On-line discrimination by Mahalanobis distance). Its performance was also compared against three existing methods: (i) SVM proposed by Guerrero et al. (2012) based on support vector machines, (ii) AES proposed by Montalvo et al. (2013) applying a double thresholding and morphological operations and (iii) LVQ proposed by

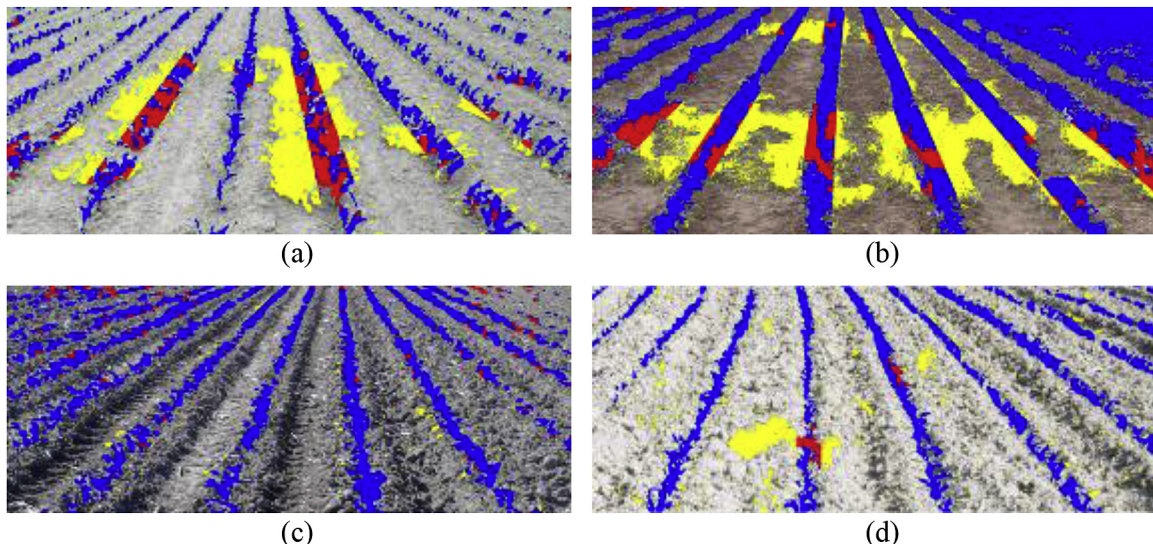


Fig. 13 – Examples of images with the crop/weed identification by using the Mahalanobis distance and majority filtering with size 7×7 from images in Fig. 1. Crop plants are labelled in blue, intra-row weeds in red and inter-row weeds in yellow.

Table 4 – Confusion matrices and Kappa coefficients for an illustrative image with 7×7 filtering.

Classifier	TP	FN	FP	TN	Number of pixels	Kappa
Mahalanobis	48132	1261	5247	22623	77263	0.81
Euclidean	43765	5757	5062	22679	77263	0.70

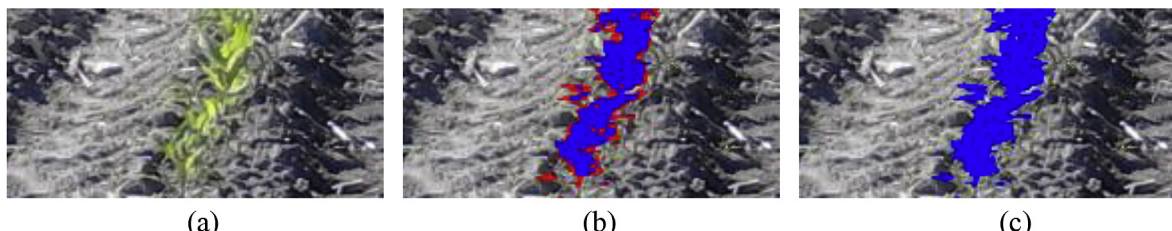


Fig. 14 – Example of classification; (a) RGB sub-image; (b) and (c) without and with refinement, respectively.

Montalvo et al. (2012b) using a double thresholding and learning vector quantisation. All methods were implemented in Matlab. Table 5 shows the percentages of successes obtained for the mentioned approaches on the tested images. From these results, it can be seen that ODMD (91.8%) outperforms the existing methods, but with a similar value than AES. Furthermore, ODMD achieves two important advantages against the three approaches: (i) the training phase is performed on-line (Fig. 7), unlike SVM, AES, and LVQ methods where exhaustive training is carried out off-line; (ii) the testing phase identifies separately both inter- and intra-row weeds (Fig. 10a).

The computational cost of the Mahalanobis classifier was also computed. Table 6 shows the average processing times in percentage (%) and milliseconds (ms) of automatic method divided by modules. The execution time for the full process was 280 ms. The segmentation module consumes the 43.5% of total time, training 15.4% and testing 41.0%. The Mahalanobis approach has proved to be, on average, 12% more computationally expensive than Euclidean procedure. This is due to the extra mathematical operations required to compute the co-variance matrices (Eqs. (6) and (7)).

In addition, it must be considered that the running time was measured in Matlab using an interpreted programming language. It may decrease significantly implementing the method by using a compiled programming language (e.g. C++) and running on a real-time platform and operating system, e.g. LabView and CRio as in the RHEA (2014) project. Under this implementation the processing time could be reduced about the 40%, as reported in RHEA, improving considerably the performance, which could be useful for real-time applications and it is a topic for a future research. In this regard in RHEA was established that a tractor navigating at speeds of 6 km/h, each image must be processed with times below 1.8 s, i.e. the proposed approach (ODMD), including the required crop row detection process (García-Santillán et al., 2017b), is below these processing times.

Finally, regarding limitations of the ODMD method, three constraints should be considered for its application: (i) the method requires previous crop rows detection process; (ii) the application at initial growth stages (up to 40 days) because of

maize leaves extend beyond the margins of crop after this stage, which can be incorrectly identified as inter-row weeds, getting worse the performance; (iii) the crop breadth estimation is manually set according to the plants growth stage (Fig. 5). The margin (value) at the base of the ROI could be automatically obtained in future works.

4. Conclusions

The present study proposes a new automatic computer vision method to discriminate crop/weed in maize fields for initial growth stages (up to 40 days) of plants based on the Mahalanobis distance as a spectral similarity metric, considering both straight and curved crop rows. The method can be part of a perception system installed on board autonomous vehicles able to navigate through the crops in real time and to carry out an effective control of weeds by applying site-specific treatments. The method consists of three on-line phases: segmentation, training and testing, Fig. 3.

The proposed method has proven to be suitable under uncontrolled lighting conditions (Fig. 1) by using a colour camera installed on the front of a tractor with imaging perspective projection. It has been tested with different weed pressures, which are irregularly distributed in the inter- and intra-row spacing. The method identifies crops plants and also both inter and intra-row weeds (Fig. 13).

The use of the Mahalanobis distance outperforms the Euclidean one (Fig. 10) with a little extra computational time. Majority filtering with size 7×7 works appropriately, achieving accuracy of 91.8% and Kappa coefficient of 0.77 (Table 2), fulfilling the requirements of commonly accepted values (see Table 3) and it is in accordance with the performances of three existing methods (Table 5) with improvement, as well as with a suitable processing time always lower than 280 ms (Table 6).

Conflicts of interest

None.

Acknowledgments

The research has been inspired and funded partially on the RHEA project funded by the European Union's Seventh Framework Programme for Research [FP7/2007-2013] under Grant Agreement n° 245986 in the Theme NMP-2009-3.4-1 (Automation and robotics for sustainable crop and forestry management). Another part of the research leading to these results has been funded by Universidad Técnica del Norte (Ecuador).

REFERENCES

Ahmed, F., Al-Mamun, H. A., Bari, A. H., Hossain, E., & Kwan, P. (2012). Classification of crops and weeds from digital images:

Table 5 – Average percentage of successes (accuracy) obtained by SVM, LVQ, AES and ODMD.

% Successes	SVM	LVQ	AES	ODMD
Average	90.5	89.4	91.5	91.8
Rank	3	4	2	1

Table 6 – Average processing times in percentage (%) and milliseconds (ms) of automatic method divided by modules.

Modules	Mahalanobis		Euclidean	
	%	(ms)	%	(ms)
1 Segmentation	43.5	122	48.8	122
2 Training	15.4	43	12.8	32
3 Testing	41.0	115	38.4	96
TOTAL	100.0	280	100.0	250

- A support vector machine approach. *Crop Protection*, 40, 98–104.
- Astrand, B., & Baerveldt, A. J. (2005). A vision based row-following system for agricultural field machinery. *Mechatronics*, 15(2), 251–269.
- Barreda, J., Ruiz, A., & Ribeiro, A. (2009). Seguimiento visual de líneas de cultivo (visual tracking of crop rows). Thesis Master. Spain: Universidad de Murcia. Retrieved from <https://digidigitum.um.es/xmlui/bitstream/10201/22175/1/myPFC.pdf>. (Accessed 12 February 2015).
- Bossu, J., Gée, Ch., Jones, G., & Truchetet, F. (2009). Wavelet transform to discriminate between crop and weed in perspective agronomic images. *Computers and Electronics in Agriculture*, 65, 133–143.
- Brosnan, T., & Sun, D.-W. (2002). Inspection and grading of agricultural and food products by computer vision systems - a review. *Computers and Electronics in Agriculture*, 36(2), 193–213.
- Burgos-Artizzu, X. P., Ribeiro, A., Guijarro, M., & Pajares, G. (2011). Real-time image processing for crop/weed discrimination in maize fields. *Computers and Electronics in Agriculture*, 75(2), 337–346.
- Camargo-Neto, J. (2004). A combined statistical-soft computing approach for classification and mapping weed species in minimum tillage systems. Lincoln, NE: University of Nebraska.
- Castillejo-González, I. L., López-Granados, F., García-Ferrer, A., Peña-Barragán, J. M., Jurado-Expósito, M., Sánchez De La Orden, M., et al. (2009). Object and pixel-based classification for mapping crops and their agri-environmental associated measures in QuickBird images. *Computers and Electronics in Agriculture*, 68, 207–215.
- Chou, J. J., Chen, C. P., & Yeh, J. T. (2007). Crop identification with wavelet packet analysis and weighted Bayesian distance. *Computers and Electronics in Agriculture*, 57(1), 88–98.
- Congalton, R. G. (1991). A review of assessing the accuracy of classification of remotely sensed data. *Remote Sensing of Environment*, 37, 35–46.
- Davies, E. (2009). The application of machine vision to food and agriculture: A review. *The Imaging Science Journal*, 57(4), 197–217.
- Duda, R. O., Hart, P. E., & Stork, D. G. (2001). *Pattern Classification*. New York: John Wiley & Sons.
- Emmi, L., Gonzalez-de-Soto, M., Pajares, G., & Gonzalez-de-Santos, P. (2014). New trends in robotics for agriculture: Integration and assessment of a real fleet of robots. *The Scientific World Journal*, 2014, 404059, 21 pages.
- Foody, G. M. (2002). Status of land cover classification accuracy assessment. *Remote Sensing of Environment*, 80(1), 185–201.
- García-Santillán, I., Guerrero, M., Montalvo, M., & Pajares, G. (2017a). Curved and straight crop row detection by accumulation of green pixels from images in maize fields. *Precision Agriculture*, 1–24. <https://doi.org/10.1007/s11119-016-9494-1>.
- García-Santillán, I., Montalvo, M., Guerrero, M., & Pajares, G. (2017b). Automatic detection of curved and straight crop rows from images in maize fields. *Biosystems Engineering*, 156, 61–79. <https://doi.org/10.1016/j.biosystemseng.2017.01.013>.
- Gee, C., Bossu, J., Jones, G., & Truchetet, F. (2008). Crop/weed discrimination in perspective agronomic images. *Computers and Electronics in Agriculture*, 60(1), 49–59.
- Gonzalez-de-Santos, P., Ribeiro, A., Fernandez-Quintanilla, C., López-Granados, F., Brandstetter, M., Tomic, S., et al. (2016). Fleets of robots for environmentally-safe pest control in agriculture. *Precision Agriculture*, 1–41.
- Guerrero, J. M., Guijarro, M., Montalvo, M., Romeo, J., Emmi, L., Ribeiro, A., et al. (2013). Automatic expert system based on images for accuracy crop row detection in maize fields. *Expert Systems with Applications*, 40(2), 656–664.
- Guerrero, J. M., Pajares, G., Montalvo, M., Romeo, J., & Guijarro, M. (2012). Support vector machines for crop/weeds identification in maize fields. *Expert Systems with Applications*, 39, 11149–11155.
- Guijarro, M., Pajares, G., Riomoros, I., Herrera, P. J., Burgos-Artizzu, X. P., & Ribeiro, A. (2011). Automatic segmentation of relevant textures in agricultural images. *Computers and Electronics in Agriculture*, 75(1), 75–83.
- Guijarro, M., Riomoros, I., Pajares, G., & Zitinski, P. (2015). Discrete wavelets transform for improving greenness image segmentation in agricultural images. *Computers and Electronics in Agriculture*, 118(1), 396–407.
- Hague, T., Tillett, N. D., & Wheeler, H. (2006). Automated crop and weed monitoring in widely spaced cereals. *Precision Agriculture*, 7(1), 21–32.
- Ishak, A. J., Hussain, A., & Mustafa, M. M. (2009). Weed image classification using Gabor wavelet and gradient field distribution. *Computers and Electronics in Agriculture*, 66(1), 53–61.
- Kataoka, T., Kaneko, T., Okamoto, H., & Hata, S. (2003). Crop growth estimation system using machine vision. *Proceedings of the IEEE International Conference on Advanced Intelligent Mechatronics (AIM 2003)*, 1079–1083.
- Landis, J. R., & Kock, G. G. (1977). The measurement of observer agreement for categorical data. *Biometrics*, 33, 159–174.
- Mahalanobis, P. (1936). On the generalized distance in statistics. *Proceedings of the National Institute of Science*, 2(1), 49–55.
- MathWorks, Inc. (2015). *Matlab release 2015a*. Retrieved from http://www.mathworks.com/products/new_products/release2015a.html. (Accessed 3 August 2015).
- Meyer, G. E., & Camargo-Neto, J. (2008). Verification of color vegetation indices for automated crop imaging applications. *Computers and Electronics in Agriculture*, 63(2), 282–293.
- Meyer, G. E., Camargo-Neto, J., Jones, D. D., & Hindman, T. W. (2004). Intensified fuzzy clusters for classifying plant, soil, and residue regions of interest from color images. *Computers and Electronics in Agriculture*, 42, 161–180.
- Meyer, G. E., Hindman, T. W., & Lakshmi, K. (1998). *Machine vision detection parameters for plant species identification*. Bellingham, WA: SPIE.
- Midtiby, H. S. (2012). Real time computer vision technique for robust plant seedling tracking in field environment. Ph.D. Dissertation. Faculty of Engineering, University of Southern Denmark. Retrieved from http://henrikmidtiby.github.io/downloads/2012-06-13_DissertationCropWeedRecognition.pdf. (Accessed 7 September 2017).
- Montalvo, M., Guerrero, J. M., Romeo, J., Emmi, L., Guijarro, M., & Pajares, G. (2013). Automatic expert system for weeds/crops identification in images from maize fields. *Expert Systems with Applications*, 40(1), 75–82.
- Montalvo, M., Guerrero, J., Romeo, J., Oliva, D., Guijarro, M., & Pajares, G. (2012b). Unsupervised learning for crop/weeds discrimination in maize fields with high weeds densities. In *Proceedings of the International Conference of Agricultural Engineering (CIGR-AgEng2012)*, Valencia Spain (pp. 1–5).
- Montalvo, M., Guijarro, M., Guerrero, J. M., & Ribeiro, A. (2016). Identification of plant textures in agricultural images by principal component analysis. In F. Martínez-Álvarez, A. Troncoso, H. Quintián, & E. Corchado (Eds.), *Hybrid Artificial Intelligent Systems: 11th International Conference, HAIS 2016* (pp. 391–401). Seville, Spain: Cham: Springer International Publishing.
- Montalvo, M., Pajares, G., Guerrero, J. M., Romeo, J., Guijarro, M., Ribeiro, A., et al. (2012a). Automatic detection of crop rows in maize fields with high weeds pressure. *Expert Systems with Applications*, 39(15), 11889–11897.
- Montserud, R. A., & Leamans, R. (1992). Comparing global vegetation maps with the kappa statistic. *Ecological Modelling*, 62, 275–293.

- Nieuwenhuizen, A., Hofstee, J., & van Henten, E. (2010). Adaptive detection of volunteer potato plants in sugar beet fields. *Precision Agriculture*, 11(5), 433–447.
- Otsu, N. (1979). Threshold selection method from gray-level histograms. *IEEE Transactions on Systems, Man and Cybernetics*, 9(1), 62–66.
- Pajares, G., García-Santillán, I., Campos, Y., Montalvo, M., Guerrero, J. M., Emmi, L., et al. (2016). Machine-vision systems selection for agricultural vehicles: A guide. *Journal of Imaging*, 2, 34.
- Pérez, A. J., López, F., Benlloch, J. V., & Christensen, S. (2000). Colour and shape analysis techniques for weed detection in cereal fields. *Computers and Electronics in Agriculture*, 25, 197–212.
- RHEA. (2014). Proceedings of the Second International Conference on Robotics and Associated High-Technologies and Equipment for Agriculture and Forestry. In P. Gonzalez-de-Santos, & A. Ribeiro (Eds.), *New trends in mobile robotics, perception and actuation for agriculture and forestry*. Madrid-Spain: PGM. Spanish Research Council-CAR. Available on-line http://www.rhea-project.eu/Workshops/Conferences/Proceedings_RHEA_2014.pdf. (Accessed 26 July 2015).
- Ribeiro, A., Fernandez-Quintanilla, C., Barroso, J., & Garcia-Alegre, M. C. (2005). Development of an image analysis system for estimation of weed pressure. *Proceedings of the 5th European Conference on Precision Agriculture (SECPA)*, 169–174.
- Rodríguez, R., & Sossa, J. (2011). *Procesamiento y análisis digital de imágenes (digital image processing and analysis)*. Madrid, Spain: RA-MA Editorial.
- Romeo, J., Guerrero, J. M., Montalvo, M., Emmi, L., Guijarro, M., Gonzalez-de-Santos, P., et al. (2013b). Camera sensor arrangement for crop/weeds detection accuracy in agronomic images. *Sensors*, 13, 4348–4366.
- Romeo, J., Pajares, G., Montalvo, M., Guerrero, J. M., Guijarro, M., & de la Cruz, J. M. (2013a). A new expert system for greenness identification in agricultural images. *Expert Systems with Applications*, 40(6), 2275–2286.
- Romeo, J., Pajares, G., Montalvo, M., Guerrero, J. M., Guijarro, M., & Ribeiro, A. (2012). Crop row detection in maize fields inspired on the human visual perception. *Scientific World Journal*, 484390, 10 pages.
- Tellaeche, A., Pajares, G., Burgos-Artizru, X. P., & Ribeiro, A. (2011). A computer vision approach for weeds identification through support vector machines. *Applied Soft Computing*, 11(1), 908–915.
- Vidović, I., Cupec, R., & Hocenski, Ž. (2016). Crop row detection by global energy minimization. *Pattern Recognition*, 55, 68–86.
- Woebecke, D. M., Meyer, G. E., Vonbargen, K., & Mortensen, D. A. (1995). Color indexes for weed identification under various soil, residue, and lighting conditions. *Transactions of the ASAE*, 38(1), 259–269.